

Adaptive Control of high Stability with Modeling for Step-Up DC to DC Converter

* Rajender Boini, **Dr. Dharamveer mangal

*Research scholar, Department of Electrical Engineering, Sunrise university, Alwar, Rajasthan.

**Supervisor, Department of Electrical Engineering, Sunrise university, Alwar, Rajasthan.

Abstract:-

This paper explains about high frequency Stability dc-dc converter and also presents the simulation and experimental results of the Buck Boost resonant AC-Link DC-DC converter. simulation is designed in MATLAB/SIMILINK Modeling. this dc-dc converter is soft switched converter which consist resonant elements like AC inductor and AC Capacitor as a tank circuit. parallel combination of ac inductor and ac capacitor forms the ac-link., link inductor is the main device for transferring of power from input to output. link capacitor is also main device which create partial resonance with link inductor L to achieve zero voltage turn on and turn off of switches. converter has the capability to operate in buck and boost operation. it also operate in unidirectional and bidirectional operation modes. converter consist Four modes of operation which are explained in detail.

Keywords: Boost Converter, Loss Breakdown, Stability analysis DC-DC Converter.

I. INTRODUCTION

With expanding worry about vitality and environment, it is important to investigate the renewable vitality including wind power, sun oriented, energy component, and so on. Energy unit is one of promising decisions because of its favorable circumstances of zero outflow, low commotion, higher force thickness and being effectively modularized for convenient force sources, electric vehicles, appropriated era frameworks, and so forth [1]. The network associated force framework in light of energy component is demonstrated in Fig. 1. For a run of

the mill 10 kW Proton Trade Film Power device, the yield voltage is from 65 V to 107 V. In any case, the data voltage of the three stage DC/Air conditioning converter should be around 700 V, the voltage addition of the DC/DC converter between energy component and the DC/Air conditioning converter will be from 6 to 11. A high stride up DC/DC converter is required for the framework as demonstrated in Fig. 1. The DC/DC converter will produce a high recurrence info current swell, which will diminish the life time of the energy unit stack \Also the hydrogen vitality usage diminishes with expanding the present swell of the energy

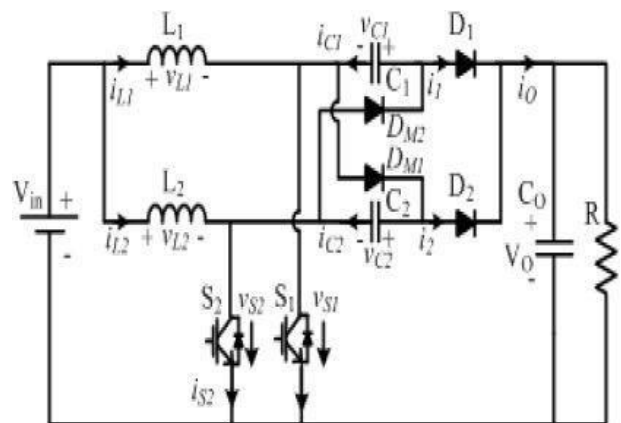
component stack yield . In this manner the DC/DC converter for the framework as demonstrated in Fig1 ought to have high stride up proportion with least information current swell. High stride up proportion can be accomplished by joining established support converter with exchanged inductors, coupled inductors, high recurrence transformer or exchanged capacitor (SC) . They can acquire high stride up proportion with high proficiency, low voltage push, and low EMI.

In request to lessen yield power module stack yield current swell or the DC/DC converter info current swell, either an inactive channel [5] or dynamic channel [5] can be utilized, then again, this will expand the unpredictability of the framework. Truth be told, interleaving the DC/DC converter can decrease the data current swell of the DC/DC converter . An interleaved help converter with voltage multiplier was proposed. Its voltage pick up was expanded up to $(M + 1)$ times (M is the quantity of the voltage multiplier) of the established help converter with the same obligation cycle D and lower voltage stress.

Other than it has lower information current swells and yield voltage swells in correlation to the traditional help converter. The interleaving help converter with voltage multipliers is demonstrated in Fig. 2. The converter indicated in Fig2 can accomplish low voltage stress in the force gadgets,

which expands the transformation productivity. On the other hand, this is just valid in overwhelming burden while the voltage anxiety of the force gadgets increments when it lives up to expectations in intermittent mode

happens when power module just supplies a light neighborhood load as demonstrated in Fig1. For this situation, higher voltage power gadgets should be utilized, and hence its expense and force misfortune will be expanded. These creators proposed another PWM control system, named as Rotating Stage Shift (APS), to conquer the issue when the converter works in light load



This paper explores a novel PWM plan for two phase interleaved support converter with voltage multiplier for Energy component Power Framework by joining APS and conventional interleaving PWM control. The APS control is utilized to diminish the voltage weight on switches in light load while the customary interleaving control is utilized to keep better execution in substantial burden. The limit

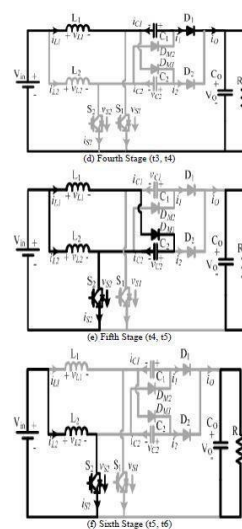
condition for swapping between APS and customary interleaving PWM control is determined. In view of the above examination, a full power reach control consolidating APS and customary interleaving control is proposed. Misfortune breakdown examination is likewise given to investigate the proficiency of the converter. At long last, it is checked by test results.

II. Boundary Condition Analysis With Traditional Interleaving Control For Low Power Operation

It is assumed that all components in the converter are ideal, both capacitor C1 and C2 are large enough, and duty cycle is less than 0.5. The operation of a switching cycle of the converter can be divided into six stages at boundary condition which the voltage stress on switch will be larger than half of the output voltage with traditional interleaving control, as shown in Fig. 3. Typical theoretical waveforms at boundary condition are shown in Fig. 4) **A. First Stage (t0, t1)** At the moment of t0, both switch S1 and S2 are off, the energy stored in the inductor L2 and capacitor C2 in previous stage are transferred to the output capacitor CO through D2 as shown in Fig. 3(a). The voltage stress on switch S1 is the input voltage Vin, and the voltage stress on switch S2 is (VO-VC2), where VO is the output voltage and VC2 is the voltage of capacitor C2.

B. Second Stage (t1, t2)

At the moment of t1, the switch S1 is turned on, the inductor L1 starts to store energy from zero as shown in Fig. 3(b). In the meantime, if $(VC1+VC2) < VO$, where VC1 is the capacitor C1 voltage, the diode D2 will be turned off, the diode DM2 will be turned on, therefore the energy in the inductor L2 will be transferred to the capacitor C1. If there is enough energy in the inductor L2, VC1 will be charged to the following state: $VC1+VC2=VO$. Then the diode D2 will be turned on again, which is shown in Fig. 5. If there is not enough energy to charge VC1 to $(VO-VC2)$, then it will come to Third Stage as shown in Fig. 3(c). If the energy in the inductor L2 is just discharged to zero and $VC1+VC2=VO$ at the end of the stage, then we call the circuit operate in boundary condition state. During the stage, the voltage stress on switch S2 is VC1.



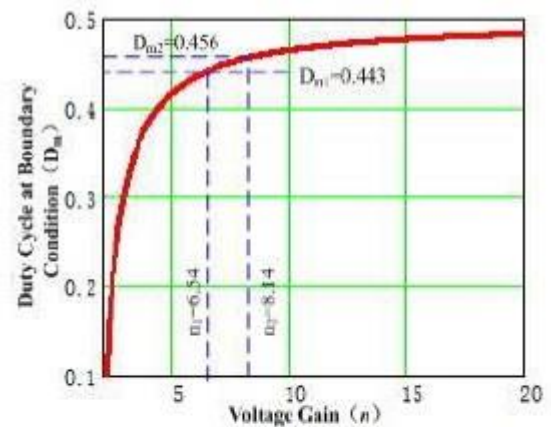
At the moment of t_5 , the current in the inductor L_1 decreases to zero. All the diodes are in off state and the inductor L_2 is in charging state until the stage comes to the end at the moment t_6 . A new switching period will begin with the next First Stage. From the above analysis, the voltage sum of capacitor C_1 and C_2 will be V_O at boundary condition. If it is less than V_O , the voltage stress on switch S_1 and S_2 will be larger than $V_O/2$, because the voltage stress on switch S_1 is $(V_O - V_{C1})$ during fourth Stage and the voltage stress on switch S_2 is $(V_O - V_{C2})$ during First Stage. The average value of the output current i_O is equal to the DC component of the load current V_O/R , then (4) Considering the same parameters of the circuit in two phases as shown in Fig. 2, therefore (5) By combining equation (4) and (5), it is derived (6) Where, R is the load. At boundary condition, the diode D_2 (D_1) approaches the conduction state during Second Stage (Fifth Stage), which is shown in. The following equation can be obtained (7) Considering both capacitor C_1 and C_2 are large enough, average voltage of the capacitor will keep equal. Otherwise, the converter will not operate at boundary condition, therefore (8) By substituting

equation (1) and (8) into equation (2), the current I_{L1M} can be derived. the total discharge of capacitor C_1 between t_3 and t_4 is The total charge of capacitor C_2 between t_4 and t_5 is According to the previous analysis, the total is charge of C_1 is equal to the total charge of capacitor C_2 at boundary condition. Therefore, there will be $Q_{c1} = Q_{c2}$ By combining equation , the following can be derived By combining and then substituting equation and into them, the boundary condition can be derived as Where, n is the voltage gain of the converter, $n = (V_o/V_{in})$. K is the parameters of the circuit and $2 / () S K = L R \times T$. The boundary constraint with traditional interleaving control decided by equation (14) is shown in Fig. 6. The constraint includes two parts: duty cycle D and the circuit parameters $2 / () S K = L R \times T$. As the switching period T_S and the input inductor L are designed at nominal operation in Continuous Conduction Mode (CCM), the constraint is determined by duty cycle D and the load R . The reason why there are two parts in the boundary constraint is that the duty cycle D varies with the load when the converter operates in Discontinuous Conduction Mode (DCM). For a given

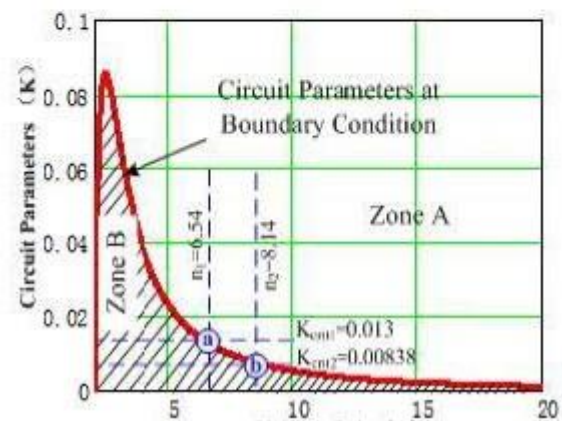
application, the voltage gain of the DC/DC converter is determined. And then the minimum duty cycle that can maintain low voltage stress in main power devices with traditional interleaving control will be given by equation (14)-(b) and as shown in Fig. 6(a).

At the same minimum duty cycle, the converter operates at boundary condition when the circuit parameters $2 / () S K = L R \times T$ satisfy equation (14)-(a) and as shown in Fig. 6(b). When the converter operates above boundary condition, the circuit parameters are in Zone A of Fig. 6(b), i.e. $K > K_{crit}$, the converter could achieve halved voltage stress on switches with traditional interleaving control with the duty cycle above the solid red line as shown in Fig. 6(a). When decreasing the load to the solid red line at boundary condition in Fig. 6(b), i.e. $K = K_{crit}$, the duty cycle of the converter will be decreased to the solid red line in Fig. 6(a). When decreasing the load further in Zone B in Fig. 6(b), i.e. $K < K_{crit}$, the duty cycle will be decreased further to be smaller than the minimum duty cycle that maintains low voltage stress on switches with traditional interleaving control. Then the APS control should be used to achieve

halved voltage stress on switches in Zone B [17, 18]. In our 1 kW prototype design, the input voltage of the converter is 86-107 V, and the output voltage of the converter is 700 V.



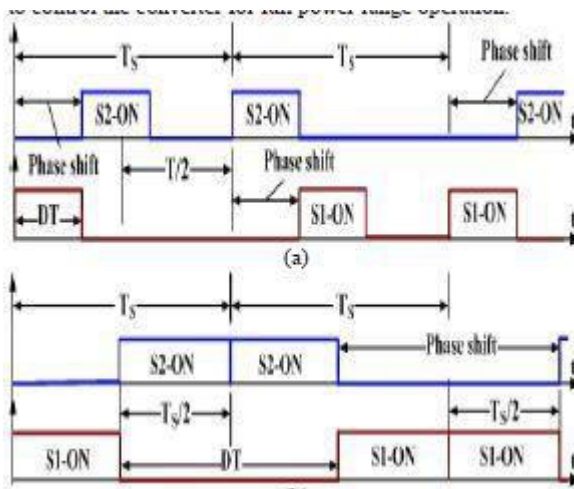
(a) Duty cycle at boundary condition varies with voltage



III. CONTROL SCHEME OF ALL POWER RANGE WITH APS AND TRADITIONAL INTERLEAVING CONTROL

According to the principle of APS [25], APS control is proposed to solve the light load

problem with duty cycle less than 0.5 as shown in Fig. 7(a). With the load increasing, the duty cycle will be increased as well. When the duty cycle is increased to 0.5, the APS control will be altered to be traditional interleaving control with halved switching frequency as shown in Fig. 7(b). According to previous analysis as shown in Fig. 6, the minimum duty cycle to achieve low voltage stress on switches with traditional interleaving control is less than 0.5. Therefore, it is possible to combine both APS control and traditional interleaving control to control the converter for full power range operation.



Considering the variation of the input voltage from 86 V to 107 V for 1 kW fuel cell operation and the output voltage of the converter 700 V, the minimum duty cycle of

traditional interleaving control varies from $D_{m1}=0.443$ to $D_{m2}=0.456$. The control scheme is shown in Fig. 8. The duty cycle is divided into three areas: $D < D_{m1}$, $D > D_{m2}$ and $D_{m1} \leq D \leq D_{m2}$. In the first area, i.e. $D < D_{m1}$, APS control will be used because traditional interleaving control cannot be effective to maintain low voltage stress on switches. In the second area, i.e. $D > D_{m2}$, traditional interleaving control will be used. In the third area, i.e. $D_{m1} \leq D \leq D_{m2}$, either APS control or traditional interleaving control may be used. In the first area ($D < D_{m1}$) with APS control and the second area ($D > D_{m2}$) with traditional interleaving control, the capacitor voltage is half of the output voltage. Therefore the switches voltage stress is clamped to half of the output voltage [17, 18]. The swapping between APS control and traditional interleaving control in the area $D_{m1} \leq D \leq D_{m2}$ is achieved by detecting the voltage stress of the switch S1 as shown in Fig. 8. When the voltage stress of the switch S1 is higher than half of the output voltage, the control is changed from interleaving control to APS control. If the traditional control is initially used in the second area ($D_{m1} \leq D \leq D_{m2}$) and once the switch S1

voltage stress is larger than half of the output voltage, the logic unit output CMP in Fig. 8 will be changed to $CMP=1$ and APS control will be enabled.

IV. SIMULATION RESULTS

A. Static Experiments In order to verify the previous analysis, prototype is built as shown in Fig. 11. The circuit parameters are as follows, $V_{in}=100$ V, $V_O=700$ V, $C1=C2=40$ μ F, $C_O=195$ μ F, $L1=L2=1158$ μ H, $T_S=100$ μ s. The load at boundary condition is $R_{BC}=2032$ Ω and $K_{crit}=0.011$ at boundary condition according to equation (14), the duty cycle D_m at boundary condition is 0.448, Fig.11. **Fig. 11.**

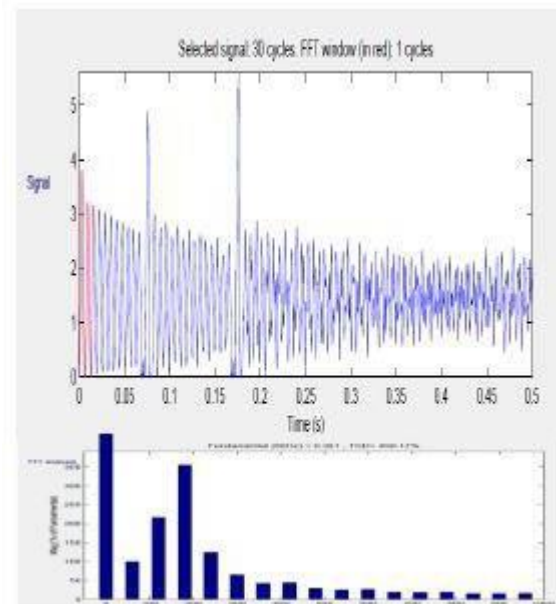
Prototype of the 1 kW Converter with Fuel Cell and Load. The simulation results at boundary condition are shown in Fig.12 which are in accordance with the theoretical waveform in Fig. 4. The simulation results are given to verify the previous analysis. With $R=478$ Ω , the output power is a bit greater than 1 kW, and $=0.049 > K_{crit}=0.013$, the converter is design to operate in Zone and the traditional interleaving control can maintain the voltage stress on switches with half of the output voltage (i.e. 350V) as With $R=1658$ Ω , i.e. $K=0.014 > K_{crit}=0.013$, the converter will continue operating in

Zone and the voltage stress on switches is still 350 V, which is about the half of the output voltage However, when decreasing the load to be 3460 Ω , i. e. $K=0.0067 < K_{crit}$, the converter will operate in Zone B of Here for comparison, two control methods are used and the results are respectively. In the traditional interleaving control is used, and we can see the voltage stress on the switch is 452 V which is higher than half of the output voltage. In Fig. 16, APS control is used, and we can see the voltage stress on the switch is 350 V which is about half of the output voltage. Therefore it is effective to use APS control when the converter operates in Zone B. With the control scheme as shown in Fig. 8, more experiments are conducted to measure the voltage stress on Power switches in all power range of the load.

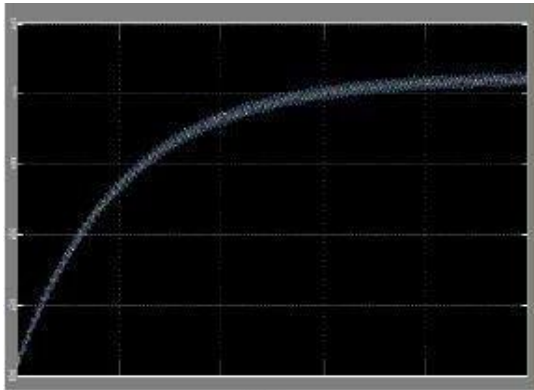
The voltage stress follows the variation of the output voltage, and almost keeps half of the output voltage in all power range. The reason why the output voltage is not stable comes from the voltage ripple of 20V in the output voltage. As the current ripple through capacitors C1 and C2 has bad effect on their lifetime and reliability, it is important to test whether the maximum current ripple is

increased when utilizing APS control.

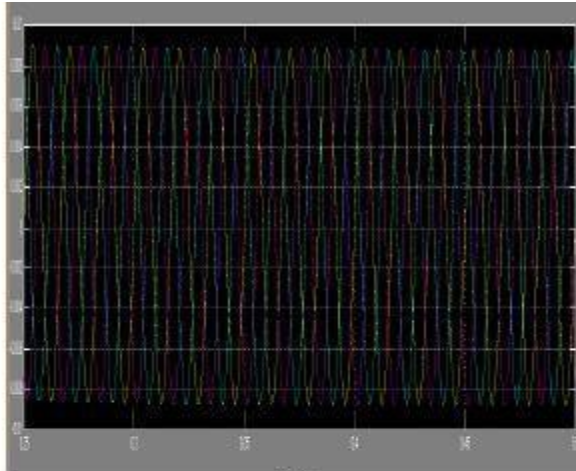
Considering the symmetry of the converter, we only test the current through C1. As shown in Fig. 18, the peak current through capacitor C1 is 3.29 A with traditional interleaving control under the load $R=3460 \Omega$, and the RMS of the current through capacitor C1 is 0.623 A. With APS control, the current ripple is not increased but reduced to be 3.21 A under the same load as shown in Fig. 19, and the RMS of the current through capacitor C1 is reduced to be 0.538 A. More experiments are conducted under different load as shown in Fig. 20, the current ripple with APS control is less than that with traditional interleaving control. Therefore, the proposed APS control can increase the lifetime and reliability of capacitors C1 and C2. The C1 and C2 are designed with film capacitor with the part number is SHB-500-40-4 from EACO Capacitor, Inc., and its maximum RMS current is 19 A, which is much greater than the above current ripple.



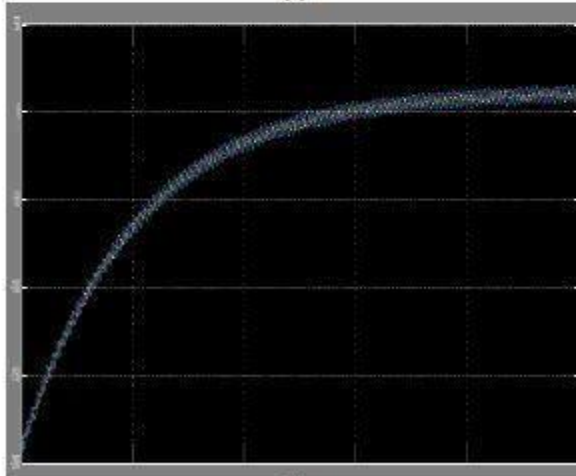
B. Dynamic Experiments In order to test the dynamic performance of the converter with fuel cell as input, the converter is connected to the output of the PEMFC shown in Fig. 11. When the load varies from 3478Ω to 1658Ω as shown in Fig. 21, the output voltage of the fuel cell will vary from 99.1V to 93.7V, the control scheme will swap from APS control to traditional interleaving



(a)



(b)



(c)

during the period of load variation, and the voltage stress of power switches keeps half

of the output voltage. When the load varies from 1658Ω to 3478Ω as shown in Fig. 22, the output voltage of the fuel cell will vary from 93.7 V to 99.1 V accordingly; the control scheme will swap from traditional interleaving control to APS control, and the voltage stress of power switches keeps half of the output voltage as well. Therefore, the control scheme proposed in this paper could achieve halved voltage stress on switches when swapping between traditional interleaving control and APS control.

V CONCLUSION

The boundary condition is derived after stage analysis in this paper. The boundary condition classifies the operating States into two zones, i.e. Zone A and Zone B. In Zone A, the traditional interleaving control is used while APS control is used in Zone B. And the swapping function is achieved by a logic unit. With the proposed control scheme, the converter can achieve low voltage stress on switches in all power range of the load, which is verified by experimental results.

VII. REFERENCES

- [1] N. Sammes, Fuel Cell Technology: Reaching Towards



- Commercialization. London: Springer-Verlag, 2006. [2] G. Fontes, C. Turpin, S. Astier, and T. A. Meynard, "Interactions Between Fuel Cells and Power Converters: Influence of Current Harmonics on a Fuel Cell Stack," *Power Electronics, IEEE Transactions on*, vol. 22, no. 2, pp. 670-678, March 2007. [3] P. Thounthong, B. Davat, S. Rael, and P. Sethakul, "Fuel starvation," *Industry Applications Magazine, IEEE*, vol. 15, no. 4, pp. 52-59, July-Aug. 2009. [4] S. Wang, Y. Kenarangui and B. Fahimi, "Impact of Boost Converter Switching Frequency on Optimal Operation of Fuel Cell Systems," in *Vehicle Power and Propulsion Conference*, 2006. VPPC '06. IEEE, Windsor, 2006, pp. 1-5. [5] S. K. Mazumder, R. K. Burra and K. Acharya, "A Ripple-Mitigating and Energy-Efficient Fuel Cell Power-Conditioning System," *Power Electronics, IEEE Transactions on*, vol. 22, no. 4, pp. 1437-1452, July 2007. [6] B. Axelrod, Y. Berkovich and A. Ioinovici, "Switched-Capacitor/Switched-Inductor Structures for Getting Transformerless Hybrid DC-DC PWM Converters," *Circuits and Systems I: Regular Papers, IEEE Transactions on*, vol. 55, no. 2, pp. 687-696, March 2008. [7] Z. Qun and F. C. Lee, "High-efficiency, high step-up DC-DC converters," *Power Electronics, IEEE Transactions on*, vol. 18, no. 1, pp. 65-73, Jan. 2003. [8] H. Yi-Ping, C. Jiann-Fuh, L. Tsorng-Juu, and Y. Lung-Sheng, "A Novel High Step-Up DC-DC Converter for a Microgrid System," *Power Electronics, IEEE Transactions on*, vol. 26, no. 4, pp. 1127-1136, April 2011. [9] L. Wuhua, F. Lingli, Z. Yi, H. Xiangning, X. Dewei, and W. Bin, "High-Step-Up and High-Efficiency Fuel-Cell Power-Generation System With Active-Clamp Flyback-Forward Converter," *Industrial Electronics, IEEE Transactions on*, vol. 59, no. 1, pp. 599-610, Jan. 2012. [10] Y. Changwoo, K. Joongeun and C. Sewan, "Multiphase DC-DC Converters Using a Boost-Half-Bridge Cell for High-Voltage and High- Power Applications," *Power Electronics, IEEE Transactions on*, vol. 26, no. 2, pp. 381-388, Feb. 2011.